

Laboratori Nazionali di Frascati

LNF-66/46

N. Abbattista, M. Coli and V. L. Plantamura : DYNAMIC BEHAVIOUR  
OF TUNNEL DIODE MONOSTABLE CIRCUITS. -

Estratto da : Nuclear Instr. and Meth. 44, 29 (1966)

DYNAMIC BEHAVIOUR OF TUNNEL DIODE MONOSTABLE CIRCUITS†

N. ABBATTISTA, M. COLI and V. L. PLANTAMURA

Istituto di Fisica, Bari, Italy and Laboratori Nazionali del CNEN, Frascati, Italy

Received 30 March 1966

The dynamic behaviour of tunnel diode monostable circuits is analysed as a function of a characteristic circuit parameter. The analysis has been developed in a general way and a special emphasis has been given to the problems of fast nuclear electronics. This analysis refers to circuits with current gain larger than one and to those performing only logic operations. It is also

comparative between circuits with linear and non linear biasing. Tunnel diode circuits biased very near to the peak have been regarded with a view to stability for multiple switching; this is in fact the most important limit for high sensitivity monostable circuits. Experimental results have been compared with theoretical calculations.

1. Introduction

The tunnel diode (td) monostable circuit, being simple and easy to realize, is most frequently used as discriminator and shaper and it is the fundamental circuit amongst those capable to perform logic functions at a repetition rate higher than 100 MHz, ref. <sup>1-21</sup>). Its properties have been generally known for a long time<sup>22</sup>.

Particular results have been given with regard to computer logic circuitry, but we are not aware of works of a greater generality whose results may turn out useful in problems of fast nuclear electronics.

The dynamic quantities considered in our analysis depend upon the parameters of the actual circuit and therefore the results are quite different from these published in works regarding the performances of the td alone<sup>23-25</sup>). The analysis has been carried out parametrically for circuits with current gain  $G_I > 1$ , or  $j_0 > 0.55^*$  and for those performing only a logic function ( $G_I < 1$ ;  $j_0 < 0.55$ ). The dynamic quantities describing in both cases the circuit performance, are the resolution time, the width and amplitude of the output signal. All of these are taken as a function of the characteristic parameter  $K = L/(R_p^2 C_1)$ . The analysis is comparative between circuits with linear bias (lb) and non linear bias (nlb); the circuits biased with a current near to the  $I_p$  value have been included and limits for multiple switching stability in the two biasing con-

ditions, have been calculated. The results carried-out in our analysis have been compared with experimental results published so far by several authors.

2. General considerations

The circuits with their equivalent schemes are shown in fig. 1a,b. The td static characteristics ( $V, I$ ) have been fitted with two parabolic functions<sup>23</sup>) joining at the point  $[1.5 V_p, f_T(1.5 V_p)]$ . The static characteristic ( $V, I$ ) of the biasing diode in fig. 1b has been fitted with two exponential functions joining at the point  $[1.5 V_p, f_D(1.5 V_p)]$ .

The normalised differential equations are the following:

a. for lb (fig. 1a)

$$\left. \begin{aligned} dv_T/dT &= j_{in} + j_0 + j_L - f_T(v_T) \\ dj_L/dT &= (E - nj_L - v_T)/K \end{aligned} \right\} \quad (1)$$

the nodal equilibrium equation at point A and the equation for the loop in which the current  $j_L$  flows respectively, with:  $K = L/(R_p^2 C_1)$ ;  $dT = dt/(R_p C_1)$ ;  $R_p = V_p/I_p$ .

b. for nlb (fig. 1b):

$$\left. \begin{aligned} dv_T/dT &= j_{in} + j_0 - f_T(v_T) \\ dv_D/dT &= [j_B - j_L - f_D(v_D)](C_1/C_2) \\ dj_L/dT &= (v_T - v_D)1/K \end{aligned} \right\} \quad (2)$$

the nodal equilibrium equations at points A, B and the differential relation for the current  $j_L$  in the inductance, respectively. The field of variability chosen for  $K$  is between 20 and  $10^4$  being this the only one of practical meaning. The sets of eqs. (1) and (2) have been solved with the aid of a digital computer.

3. Methods of analysis with  $G_I > 1$

A set of calculations has been worked out with td biased with  $j_0 = 0.9$  which is the maximum value

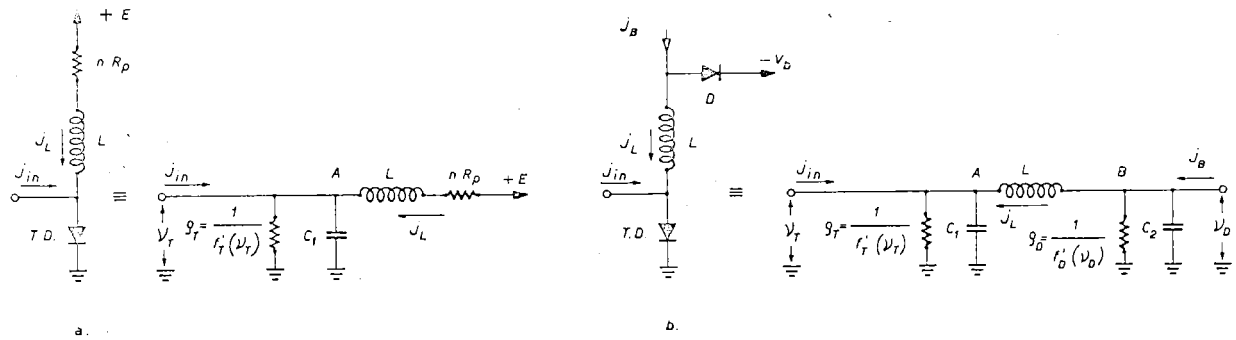
† Work in part supported by C.N.R.

\* The current gain  $G_I$  is defined as

$$G_I = \{f_T(v_{max}) - j_v\}/j_{in}$$

where:

- $f_T(v) = j$  = the td current normalised to the peak current  $I_p$ ;
- $v_{max}$  = the maximum value of the voltage, during the dynamic cycle of the circuit, normalised to the peak voltage  $V_p$ ;
- $j_v$  = the normalised value of the current at the valley point;
- $j_{in}$  = normalised input current;
- $j_0$  = normalised biasing current;
- $K$  = parameter as defined in section 2.



$$v = \frac{V}{V_p} \quad j = \frac{I}{I_p}$$

$$R_p = \frac{V_p}{I_p}$$

$$r_T(V_T) \equiv \begin{cases} -V_T^2 + 2V_T & \text{for } V_T < 1.5 V_p \\ 0.1625 V_T^2 - 1.1375 V_T + 2.0906 & \text{for } V_T > 1.5 V_p \end{cases}$$

$$r_D(V_D) \equiv \begin{cases} e^{T_1 V_D} - 1 & \text{for } V_D < 1.5 V_p \\ e^{T_2 (V_D - 1.5)} - 0.95 & \text{for } V_D > 1.5 V_p \end{cases} \quad \text{and} \quad \begin{cases} T_1 = \frac{1}{1.5} \log 1.05 \\ T_2 = \frac{1}{1.95} \log 1.95 \end{cases}$$

$g_T \equiv \text{Dynamic resistance of T.D}$   
 $g_D \equiv \dots \dots \dots D.$

Fig. 1. Tunnel diode monostable schemes; a. linear bias, b. non linear bias.

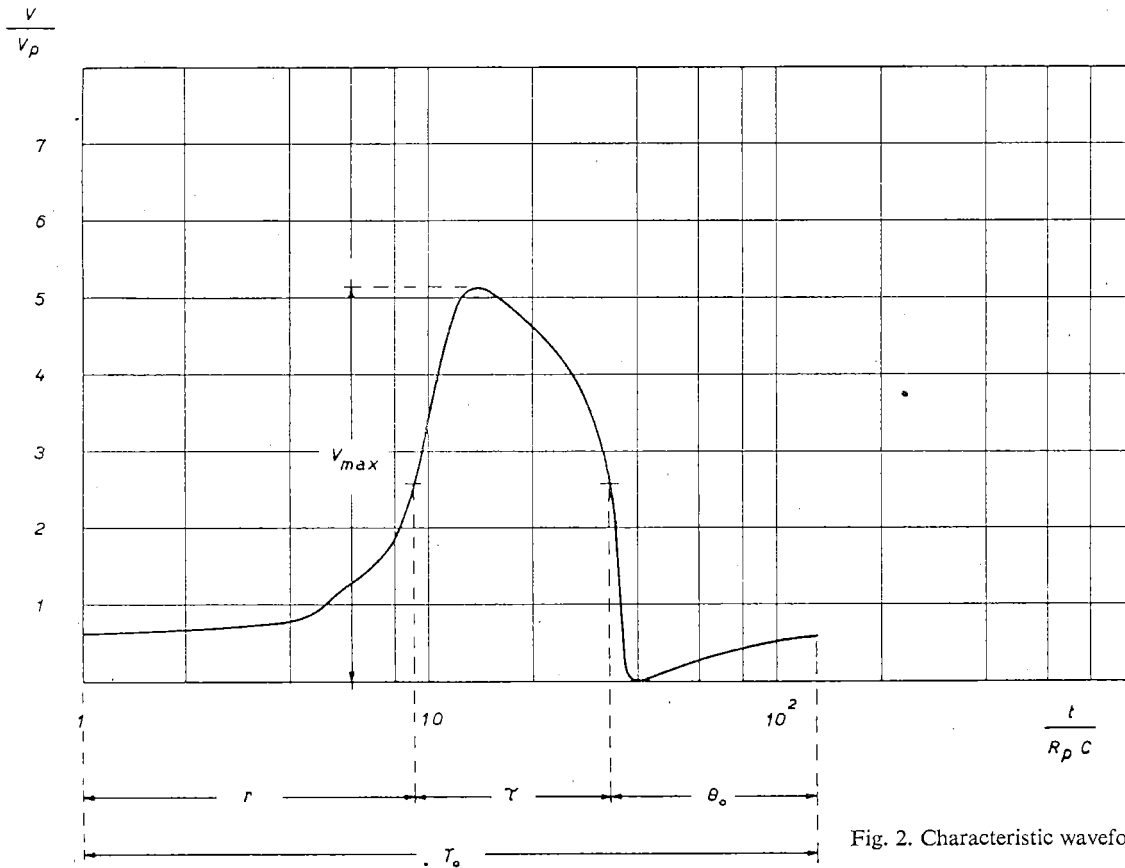


Fig. 2. Characteristic waveform.

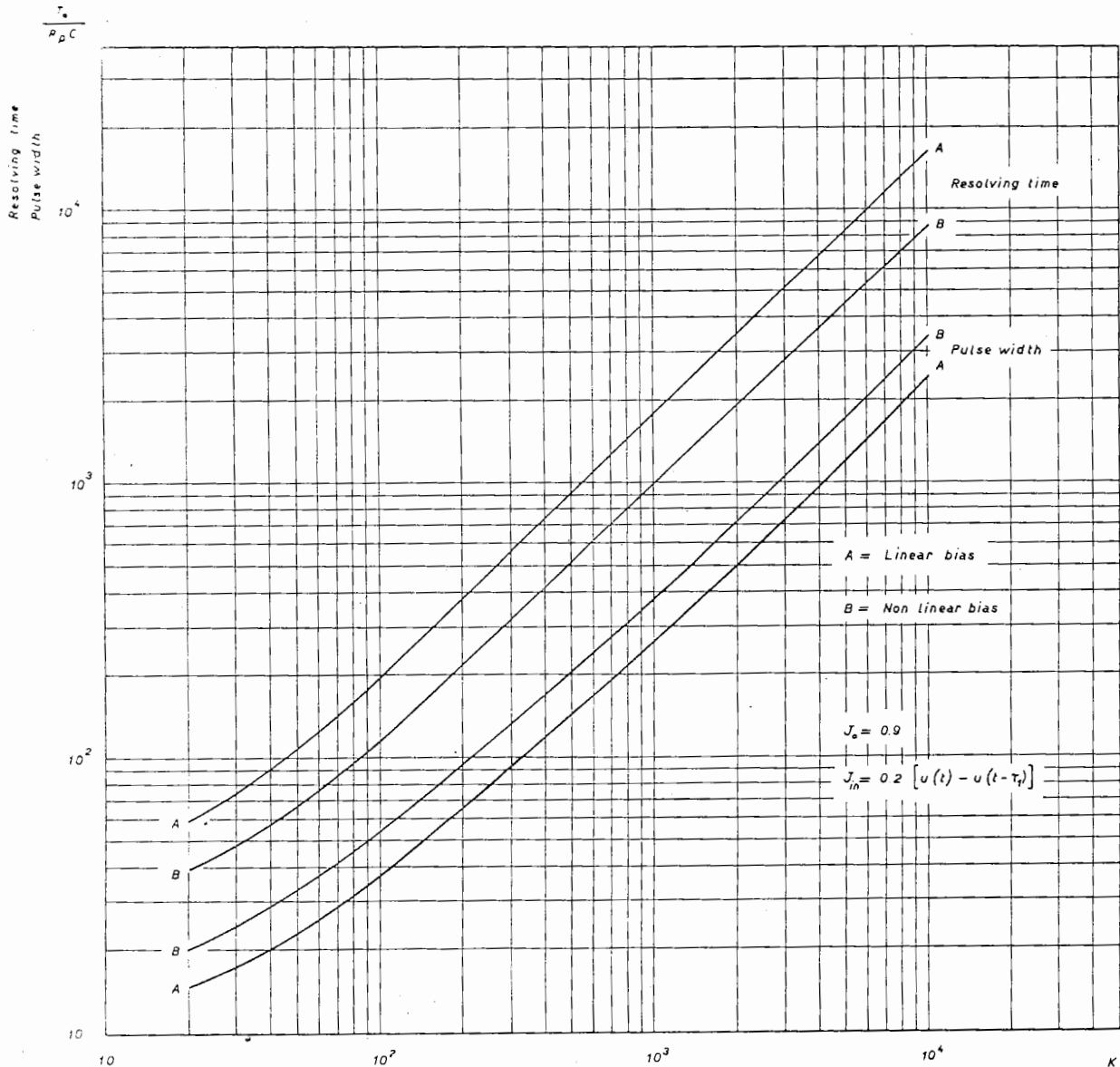


Fig. 3. Resolving time and width vs  $K$ .

allowed by tolerance considerations for maximum  $G_T$ , ref. 25). Output waveforms have been obtained for an input triggering pulse  $j(t) = j_{in}[u(t) - u(t - \tau_1)]$  where  $\tau_1$  is the minimum allowed width to fire the td. For a better understanding of the dynamic quantities we refer in fig. 2 to a typical voltage waveform:

- a.  $T_0$  = the total duration of the dynamic cycle ( $v, j$ ) from the biasing point  $(v_0, j_0)$  to the quiescent point  $\{v_0 \cdot (1 - 0.01), f_T[v_0 \cdot (1 - 0.01)]\}$ ;
- b.  $A_0$  = the input pulse amplitude normalized to  $I_p[A_0 = j_{in}]$  with 10% overdrive\*;
- c.  $\tau$  = the output width measured at fwhm;

- d.  $\theta_0$  = the dead time measured on the trailing edge from fwhm to the quiescent point;
- e.  $\delta$  = the duty cycle, defined as:  $\delta = \tau/T_0$ .

3.1. RESOLVING TIME VS  $K$

The resolving time vs  $K$  is shown in fig. 3 for lb and nlb. It has been defined ( $= T_0$ ) as the minimum delay between two equal amplitude input pulses. For  $K > 10^2$  the ratio between operation rates for nlb and lb is approximately 1.8.

\* Overdrive =  $j_{in} + j_0 - 1$ .

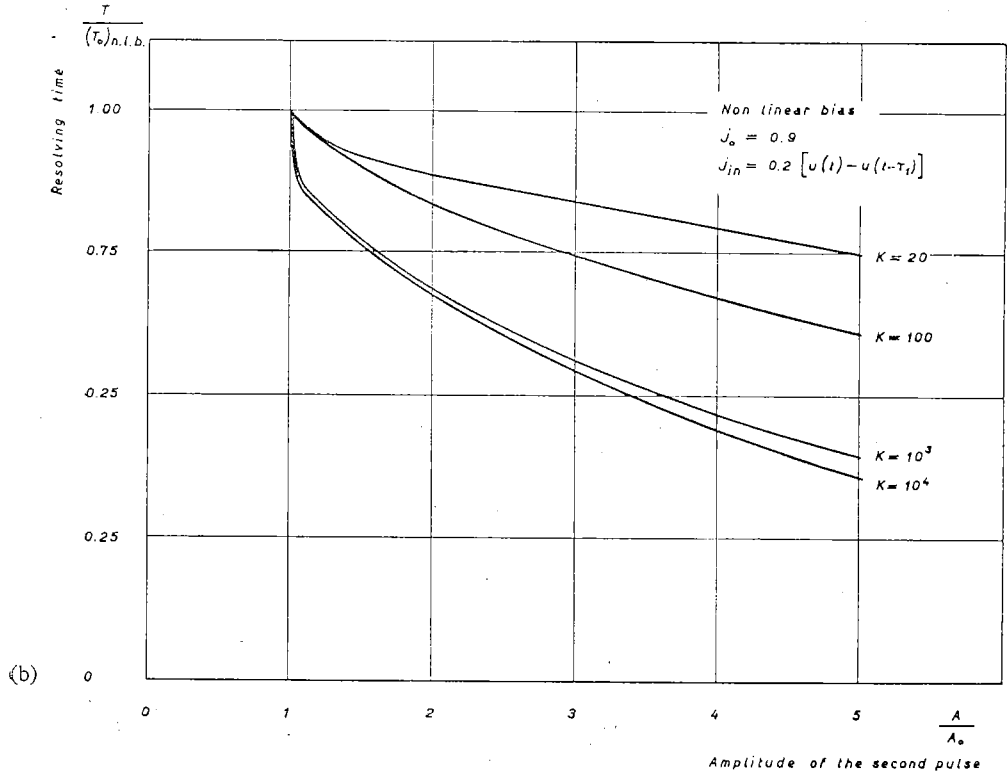
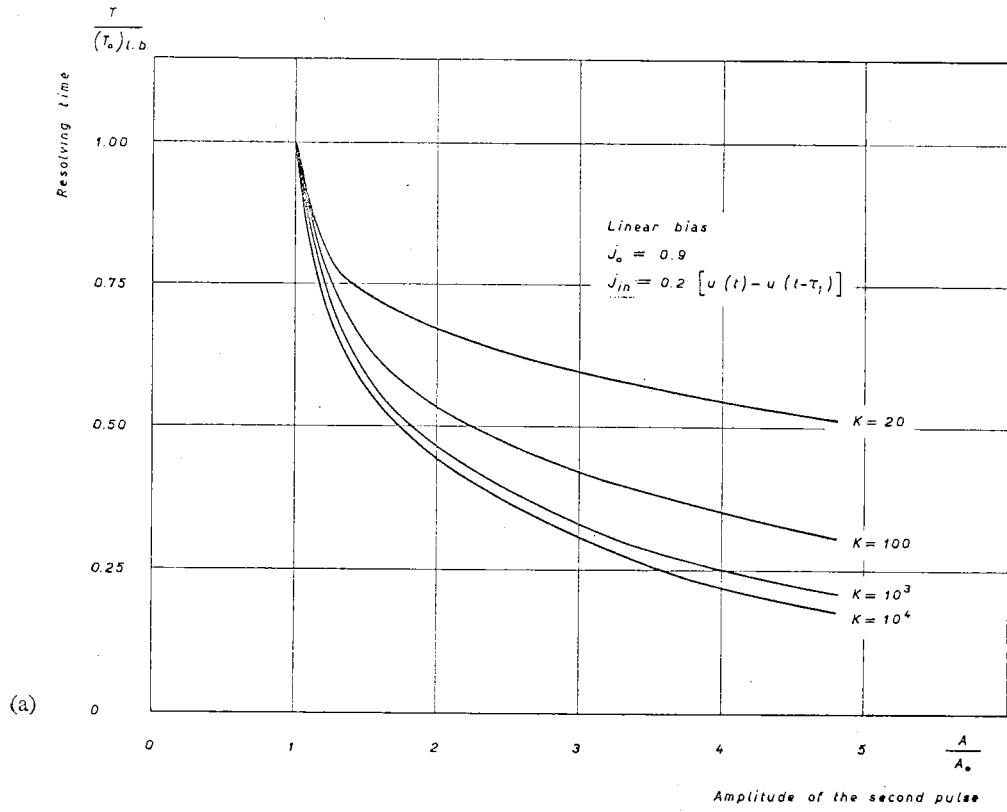


Fig. 4. Resolving time vs amplitude of the second pulse.

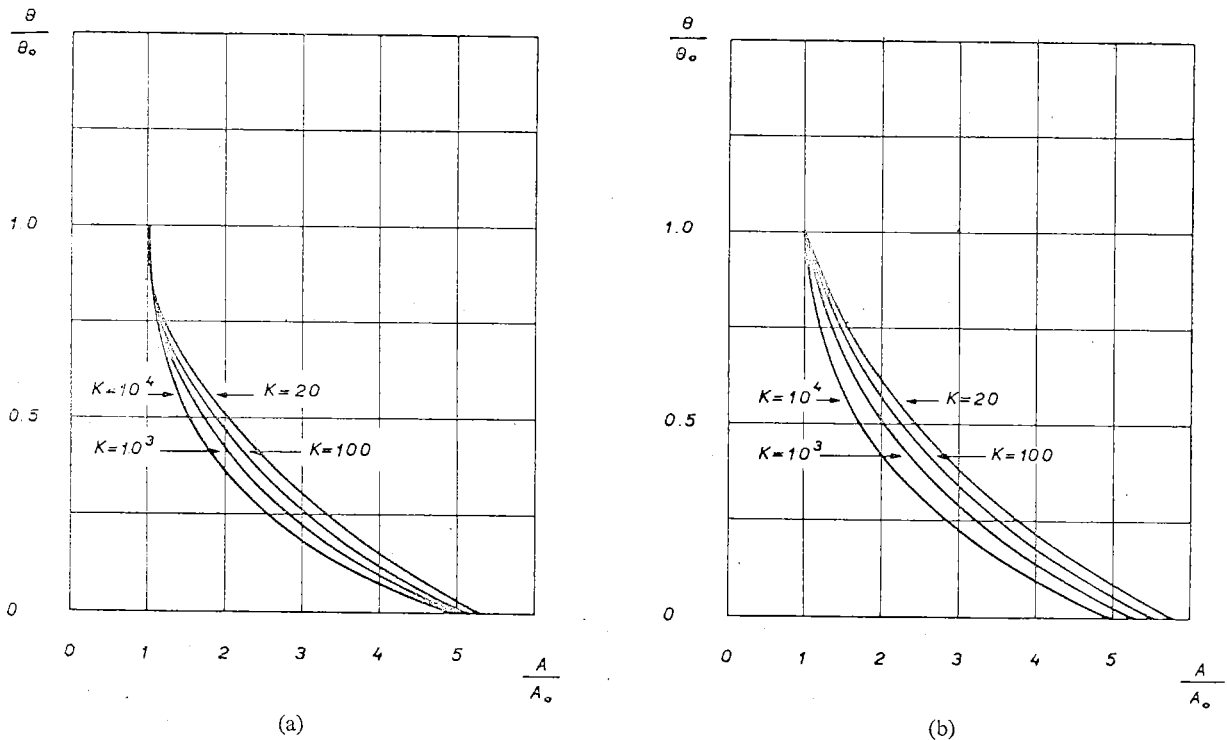


Fig. 5. Dead time vs amplitude of the second pulse; a linear bias; b. non linear bias.

### 3.2. OUTPUT PULSE WIDTH VS $K$

For the same value of  $K$  the output pulse width (fig. 3) in the case of nlb is always larger than that for lb; the width and the resolving time for nlb are contained between the curves for the lb. This can be summarized saying that the duty cycle is 40% for the nlb and 20% for the lb. For low values of  $K$  the curves show a lower value for the duty cycle  $\delta$ , which is in good agreement with experience. To have the same width, different values of  $K$  must be chosen ( $K_{nlb} < K_{lb}$ ). This brings in turn a further increase for the ratio of the operation rates with advantage for the nlb circuit.

### 3.3. RESOLVING TIME VS AMPLITUDE OF THE SECOND INPUT PULSE

The diagrams in fig. 4 show the resolving time,  $T$ , normalized to  $T_0$ , for two input pulses, vs the amplitude of the second input pulse,  $A$ , normalised to the amplitude  $A_0$  (0.2 for our case) of the first pulse. The amplitude needed to reduce the resolving time for the nlb is greater than that needed for the lb. In fact the increase of amplitude of the second pulse reduces only the dead time that is already little for the nlb.

The diagram of the dead time  $\theta$ , normalised to  $\theta_0$ ,

\*  $V_{pD}$  is the projected peak voltage of the actual td.

for the two cases of biasing, is reported in fig. 5 vs the ratio  $A/A_0$ .

### 3.4. MAXIMUM OUTPUT PULSE AMPLITUDE VS $K$

The output amplitude, normalised to  $V_p$ , vs  $K$  is shown in fig. 6. The scale factor  $S_t = 5.88 V_p/V_{pp}^*$  matches the static characteristic ( $V, I$ ) of the actual td to the ideal one.

The normalised projected peak voltage has been assumed for the calculation as  $v_{pp} = 5.88$ . It can be noted that for  $K=20$  the output amplitude is nearly equal to the valley voltage  $v_v$ , that is the pulse is useless for practical applications. For equal output pulse amplitude the value of  $K$  for nlb is lower than that for lb; therefore one can at once deduce that the operation rate for the nlb is higher. With useful output amplitude the circuit with nlb allows to reach an operation rate not otherwise attainable.

### 3.5. PARAMETER $W$ VS OUTPUT SIGNAL AMPLITUDE

It may be meaningful to consider the product  $W$ , (output signal amplitude  $\times T_0^{-1}$ ), since it may be taken as a parameter to compare the monostable circuits in the two biasing conditions considered. The plot of  $W$ , vs the output signal maximum value, is shown in fig. 7. It is useful to find the value of  $R_p C_1$ , that is to choose

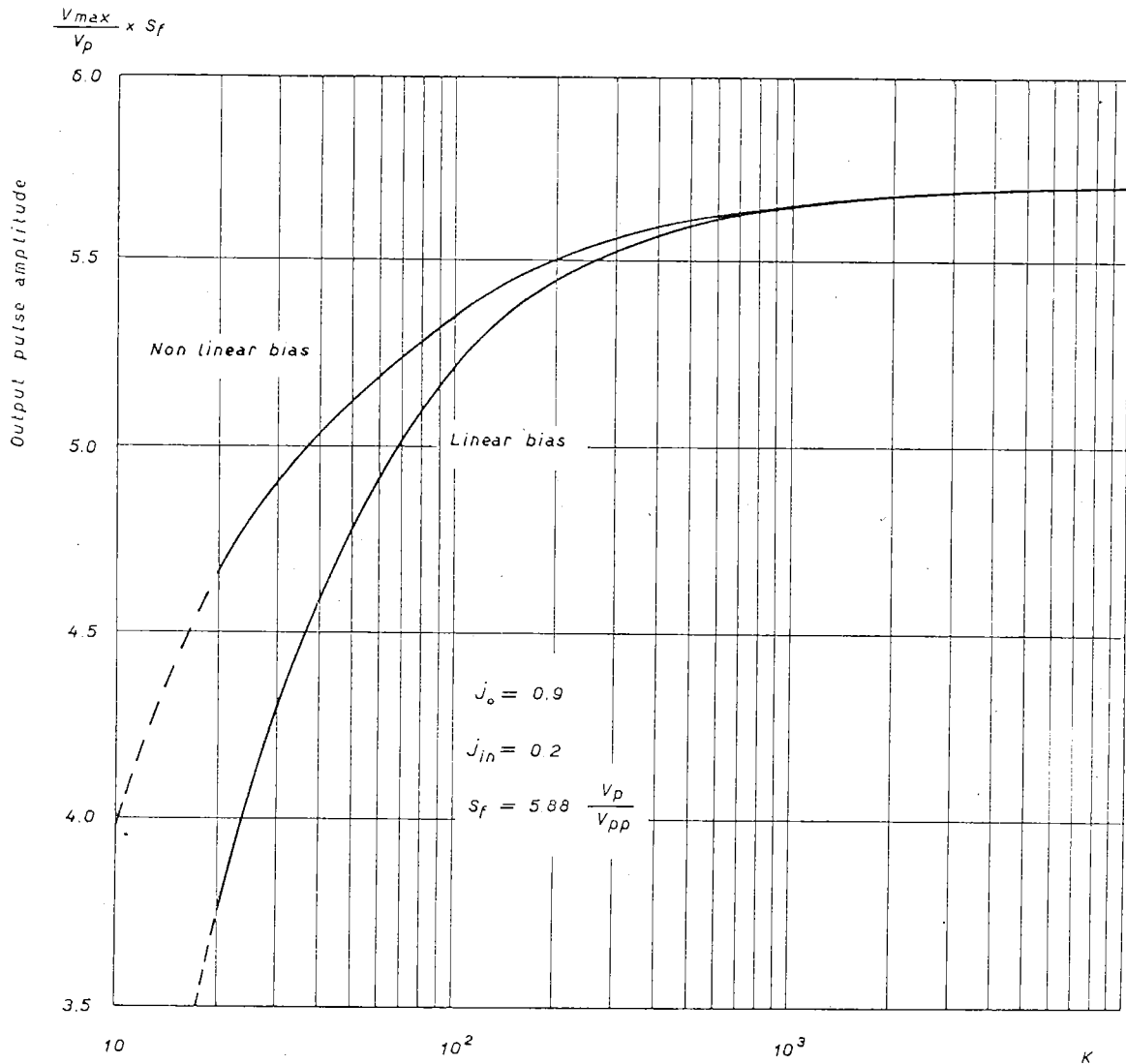


Fig. 6. Output pulse amplitude vs  $K$ .

the  $td$ . It can then furnish the maximum value of the output signal obtainable when the operation rate has been fixed.

**4. Monostable circuits with  $G_I < 1$**

We have considered the biasing conditions  $j_0 = 0$  and  $j_0 = -1$ . In these conditions it is impossible to find a point\* on the negative resistance region of the  $td$  where a switching regenerative action may continue once the input current has been removed. Infact the  $j_L$  current is, in each point, lower than that needed by the  $td$ .

\* This point is defined by the following relations:

$$d(j_{in} + j_L)/dv_T = df_T(v_T)/dv_T; \quad j_L > f_T(v_T).$$

The input waveforms may be represented by:

$$j(t) = j_{in}[u(t) - u(t - \tau_2)],$$

where  $\tau_2$  is the input pulse width which is maintained as long as the output voltage is risen to its maximum. The dynamic quantities have been gathered in table 1 for lb and in table 2 for nlb. Generally we can say that, when  $j_0$  is lowered, the voltage step across the inductance increases. As a result, when  $j_0 < 0.55$  ( $G_I < 1$ ) the output pulse width depends from the circuit ( $K$ ) but strongly from the biasing point, so that the signal width becomes very short. If the input signal is longer than  $\tau_2$ , the circuit behaves as that with  $G_I > 1$ . In fact the input current must be added to the biasing one.

TABLE 1  
 Linear bias, for  $j_0 = 0$  and  $j_0 = -1$ .

	$K$	Maximum amplitude ( $V_p$ )	Rise time ( $R_p C_1$ )	Width ( $R_p C_1$ )	Dead time ( $R_p C_1$ )	Resolution time ( $R_p C_1$ )
$j_0 = 0$	20	—	—	—	—	—
	$10^2$	5.43	18	10.6	2.3	25
	$10^3$	5.90	18	16.9	5.6	32
	$10^4$	5.96	18	22.2	7.8	39.4
$j_0 = -1$	20	—	—	—	—	—
	$10^2$	5.76	11.6	8.8	1.9	15.2
	$10^3$	5.89	16.7	9	2.6	21.5
	$10^4$	5.96	18.2	10.9	3	23.5

 TABLE 2  
 Non-linear bias, for  $j_0 = 0$  and  $j_0 = -1$ .

	$K$	Maximum amplitude ( $V_p$ )	Rise time ( $R_p C_1$ )	Width ( $R_p C_1$ )	Dead time ( $R_p C_1$ )	Resolution time ( $R_p C_1$ )
$j_0 = 0$	20	5.0	17	7.8	2	22
	$10^2$	5.62	17	11.4	2.5	25
	$10^3$	5.9	17	18.8	6	34
	$10^4$	5.96	17	24.4	8	41.6
$j_0 = -1$	20	4.98	18	6.7	1.5	22
	$10^2$	5.6	18	8.23	2.1	23.4
	$10^3$	5.9	18	10.7	2.9	23.4
	$10^4$	5.96	18	13.2	3	25.8

### 5. Analysis of the stability for biasing current near to the peak ( $I_p$ ).

The lowest threshold of a switching circuit is determined by two factors: a. the noise; b. the overshoot after the switching transients, which is as more dangerous as lower is the threshold. We want to calculate the lowest threshold value keeping into account the contribution from the two limitations cited above.

#### 5.1. STABILITY FOR NOISE CURRENT

It is well known<sup>26)</sup> that the intrinsic noise current of a td may be expressed by:

$$i_r^2 = 4kTg_c \Delta f,$$

where:

$$g_c = [r_s + g_d / \{g_d^2 + (\omega C_1)^2\}]^{-1},$$

$r_s$  = the td series resistance;

$k$  = the Boltzmann constant;

$g_d$  = the equivalent conductance of a td at the biasing point.

For  $j_0 \approx 1$ ,  $g_d \geq 0$ . Assuming  $r_s = 1\Omega$  we can write:

$$i_r = 2(kT\Delta f)^{\frac{1}{2}},$$

whose value for  $\Delta f = 10^{10}$  Hz,  $T = 300^\circ\text{K}$  is  $12\ \mu\text{A}$ . Disregarding the effect of the equivalent conductance of the current generator  $i_r$ , we see that, in the case of  $I_p = 10^{-2}$  A, the highest value allowed for  $j_0$ , regarding only the noise limitations, is  $j_0 = 0.999$ .

For low level discrimination, td with  $I_p = 10^{-3}$  A are commonly used. As a result we can hold that, with some safety factor, the highest allowable value of  $j_0$  is 0.99.

#### 5.2. STABILITY OF LB CIRCUITS

On the basis of experimental work<sup>27)</sup> we assume in this case the equivalent circuit of fig. 8a in which:

$R_1 = mR_p$  is the td differential resistance at the biasing point;

$C_1$  the td capacitance, assumed constant and equal to the value of the td valley capacitance.

The characteristic determinant of the circuit gives, for critical damping, the following condition:

$$(R_1 R_2 C_1 + L)^2 - 4LR_1 C_1 (R_1 + R_2) \geq 0,$$

from which substituting the defined parameters, we obtain:

$$|(\sqrt{K/m}) - (n/\sqrt{K})| \geq 2. \quad (3)$$

With the parabolic approximation assumed for the td static characteristic:

$$m = \frac{1}{2}(1 - j_0)^{-\frac{1}{2}}. \quad (4)$$

The relation (3) is plotted in fig. 9a for  $n = 2$ . It gives the gap of forbidden values of  $K$  vs the biasing current. For biasing current  $j_0 < 0.99$ , which is the noise limit assumed above, we can state that the condition (3) does not impose further limitation for the allowable values of  $K$ .

#### 5.3. STABILITY OF NLB CIRCUITS

On the basis of the equivalent circuit in 5.2, linearising the resistance of the biasing diode, we obtain the circuit in fig. 8b. Noting that  $R_1 C_1 \ll R_2 C_2$  we can disregard  $C_1$ . As in <sup>27)</sup> we think the inductance as an ideal buffer during the back-switching of the td. We can then assume that the biasing diode is behind the knee of its characteristic and put approximately  $R_2 \approx 30 R_p$ , as we have calculated from the exponential approximation given in fig. 1.



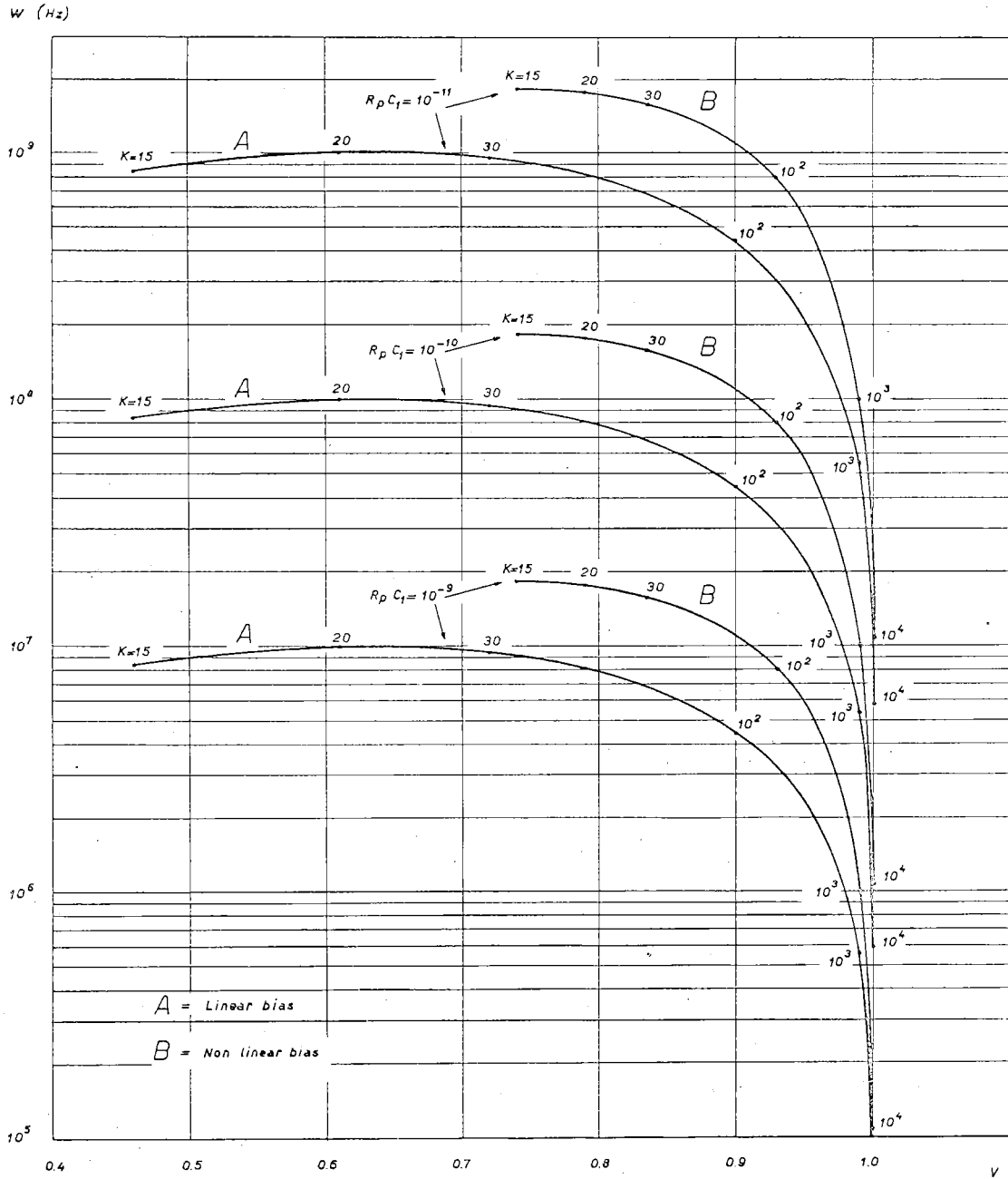


Fig. 7. *W* factor vs *V*.

The critical damping condition, the same as (3), is:

$$|(\sqrt{K}/n') - (m'/\sqrt{K})| \geq 2,$$

where:

$$n' = n/\sqrt{c}; \quad m' = m/\sqrt{c}; \quad c = C_1/C_2.$$

Regarding eq. (5) we find that the two roots  $K_1$  and  $K_2$  vary proportionally to  $1/c$ . We can now obtain precise values of  $m$  from eq. (4), but the evaluation of

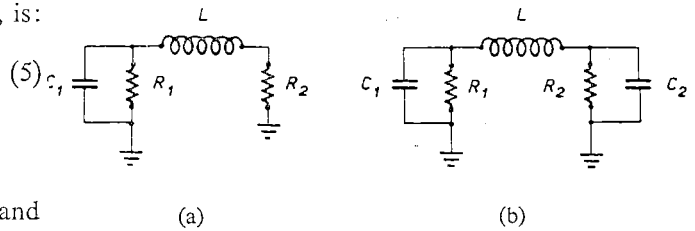


Fig. 8. Equivalent circuit from the idealized characteristics a. linear bias; b. non linear bias.

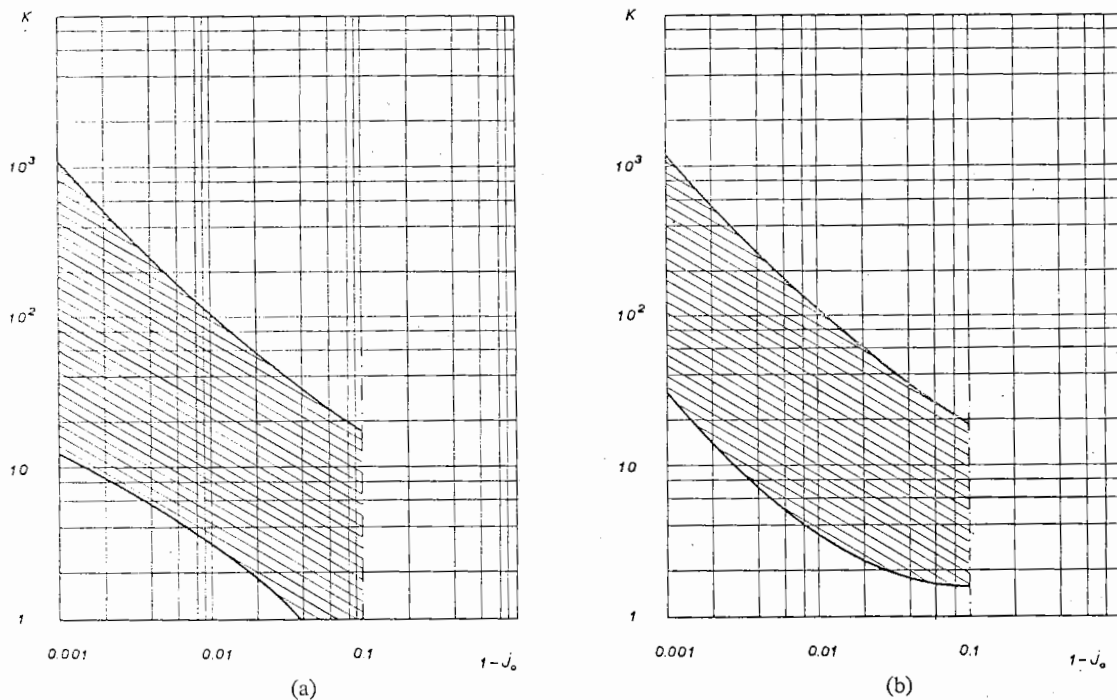


Fig. 9.  $K$  forbidden values: a. linear bias; b. non linear bias.

$n$ , vs the biasing current, remains problematic. Since the inductance differs very much from an ideal buffer, the hypothesis assumed above will give roughly approximated results. Then we are allowed without wasting more calculations, to hypothesize a variation of  $n$  proportional to  $m$ .

The relation (5) is plotted in fig. 9b, for  $c = 1$ . For  $j_0 < 0.9$  it is not necessary to impose critical damping conditions to assure stability to the circuit.

For  $0.9 < j_0 < 0.99$  the values of  $K$  between the forbidden gap are cautelative because little overshoots may be allowed. This cannot be repeated for the values of  $K$  corresponding to  $j_0 > 0.99$ , being now important the contribution of noise.

### 5. Comparison with experimental results

We have examined many published results which are in agreement with our calculations, as can be seen from the following example:

Referring to <sup>16)</sup> we have verified the points on the diagrams in fig. 5–7. For fig. 6 (dead-time vs inductance) we find a satisfactory agreement, considering that in such figure the results are given for the 90% of the recovery time. For fig. 5 (output pulse width vs inductance) and fig. 7 (pulse height vs inductance) the behaviour is the same as in our fig. 3 and 6.

The absolute values are a little different on account of the fact that the monostables considered in <sup>16)</sup> are

realised with gallium arsenide diodes loaded by a germanium diode that is a very heavy load<sup>28)</sup>. Many experimental results, obtained with different types of td (GaAs and Ge, fast and slow types) and for several values of  $K$  have been compared with the expected results from the diagrams, showing an agreement within 10%.

The helpful assistance of Prof. M. Merlin and the encouragement of Prof. G. Giannelli are greatly acknowledged.

### References

- 1) T. A. Rabson, Nucl. Instr. and Meth. **12** (1961) 127.
- 2) A. Adler, M. Palmi and V. Perez Mendez, Nucl. Instr. and Meth. **13** (1961) 197.
- 3) S. Gorodetzky, A. Muser, J. Zev and R. Armbruster, Nucl. Instr. and Meth. **13** (1961) 282; **14** (1961) 205.
- 4) D. McGervey, Nucl. Instr. and Meth. **14** (1961) 351.
- 5) R. Van Zurk, Nucl. Instr. and Meth. **16** (1962) 157.
- 6) F. Pandarese and F. Villa, Nucl. Instr. and Meth. **20** (1963) 319.
- 7) E. Baldinger, Nucl. Instr. and Meth. **20** (1963) 309.
- 8) P. R. Orman, Nucl. Instr. and Meth. **21** (1963) 121.
- 9) C. B. Ward and C. M. York, Nucl. Instr. and Meth. **23** (1963) 213.
- 10) T. Hvam and M. Smedsdal, Nucl. Instr. and Meth. **24** (1963) 55.
- 11) S. Kullander, Nucl. Instr. and Meth. **24** (1963) 342.
- 12) U. Sold and S. Brojdo, Nucl. Instr. and Meth. **26** (1964) 147.
- 13) A. Adin and B. Sabbah, Nucl. Instr. and Meth. **26** (1964) 355.